Indian Journal of Chemistry
Vol. 59A, March 2020, pp. 346-350

Thermal dehydration kinetics of non-crystalline manganese borate

Nurcan Tugrul[a,*], Ebru Firat[a], Azmi Seyhun Kipcak[a], Meral Yildirim[a], Fatma Tugce Senberber[a,b] & Emek Moroydor Derun[a]

[a]Department of Chemical Engineering, Yildiz Technical University, Turkey

[b]Civil Engineering, Nisantasi University, Turkey

Email: ntugrul@yildiz.edu.tr

Received 5 November 2018; revised and accepted 10 February 2020

In this study, non-crystalline manganese tetrahydric orthoborate ($MnH_4(BO_3)_2$) has been synthesized by using $MnSO_4.H_2O$, NaOH and H_3BO_3 via hydrothermal method. The characterizations of the synthesized compounds have been conducted using X-ray diffraction (XRD), Fourier transform infrared spectroscopy (FTIR) and scanning electron microscopy (SEM). Thermal dehydration studies have been conducted using the thermogravimetric analysis (DTG/TG). From the XRD result, it is confirmed that amorphous manganese borate is synthesized and the corresponding characteristic borate vibration are observed in FTIR spectrum shows. A particle size distribution at the micron scale with partially agglomerated state is observed from SEM images. The thermogravimetric results show that dehydration process occurs between the temperatures of 40–270 °C in one-step reaction with average weight loss of 19.26%. Average activation energies have been determined by using the non-isothermal kinetics methods of Coats-Redfern, Horowitz-Metzger and Van-Krevelen and found as 37.83, 46.54 and 37.88 kJ mol^{-1}, respectively.

Keywords: Non-crystalline, Non-isothermal kinetics, Manganese borate, Coats-Redfern, Horowitz-Metzger, Van-Krevelen

Manganese is the 12th most abundant element which constitutes about 0.098% of Earth's crust, occurs in oxides, carbonates and silicates at nature.[1,2] Materials containing manganese are used in the production of dry cell batteries, fireworks, matches, porcelain, fertilizers, livestock, supplements, varnishes, glazes and ceramics[3]. Being a sub-group of boron minerals, manganese borate is reddish-white powder used in the production of dry oils and varnishes that is insoluble in water and organic solvents.[4,5]

In literature, several studies were conducted related with manganese borates such as; Hartley and Ramage produced $MnH_4(BO_3)_2$ using the manganese sulphate and borax under vacuum between the temperatures 100-300 °C.[5] Neumair et al. prepared α-MnB_2O_4 from MnO_2 and B_2O_3 under high-pressure and high-temperature (6.5 GPa and 1100 °C)[6]. Abrahams *et al*., investigated the crystal structure, magnetization, and thermal extinction dependence of manganese diborate (MnB_4O_7).[7] Knyrim *et al.,* synthesized MnB_4O_7 using the raw materials of MnO_2 and B_2O_3 under high-pressure/high-temperature conditions of 7.5 GPa and 1000 °C.[8] Yang *et al.,* obtained $MnB_{12}O_{14}(OH)_{10}$ from $Mn(NO_3)_2$, $H_2C_2O_4$ and H_3BO_3 by two step boric acid flux method where in first step reactants were reacted at a reaction temperature of 150 °C for 2 days and in the second step intermediate product was heated at 220 °C for 3 days.[9] Svirko and Boiko, investigated the infrared absorption spectra of manganese borates.[10] Norrestam *et al.,* synthesised manganese oxyborate from MnO_2 and B_2O_3 at 800 °C.[11] From the literature it is seen that in both solid-state (thermal) and liquid-state (hydrothermal) methods, the reaction is depending on high-pressure/high-temperature.

Decomposition process of hydrated minerals begins with the removal of crystal water and keeps on with the removal of hydroxyl ions as water molecules from the structure. These stages of decomposition are defined as dehydration and dihydroxylation, respectively. Amorphization or reconstruction of dehydrated structure could be observed with increasing temperature.[12] In the literature; the thermal dehydration behavior and kinetics of boron mineral and compounds such as borax ($Na_2B_4O_7{\cdot}10H_2O$)[13], tincalconite ($Na_2B_4O_7{\cdot}5H_2O$)[14], ulexite ($NaCaB_5H_{16}O_{17}$)[15], tunellite ($SrB_6H_8O_{14}$)[15, 19], howlite ($Ca_2B_5SiH_5O_{14}$)[15], lithium metaborate dehydrate ($LiBO_2{\cdot}2H_2O$)[16], sodium metaborate tetrahydrate ($NaB(OH)_4{\cdot}2H_2O$)[17], inderite ($Mg_2B_6O_{11}{\cdot}15H_2O$)[18], mcallisterite ($Mg_2(B_6O_7(OH)_6)_2{\cdot}9(H_2O)$)[20], admontite ($MgO(B_2O_3)_3{\cdot}7(H_2O)$)[21], zinc borate hydrate ($Zn_3B_6O_{12}{\cdot}3.5H_2O$)[22] and santite ($KB_5O_8{\cdot}4H_2O$)[23] have been studied.

Starting with the literature studies aforementioned, the first novelty of this study comes upon as the synthesis of manganese borates at moderate conditions for a green chemical approach, and then the second novelty comes upon as the study of thermal kinetic behavior of manganese borate which

was not studied before. Synthesized manganese borates' characterization studies were conducted by using X-ray diffraction (XRD), Fourier transform infrared spectrocopy (FTIR) and scanning electron microscopy (SEM). Thermal dehydration studies were conducted using the thermogravimetric analysis (DTG/TG).

Experimental

Synthesis of manganese borate hydrate

Manganese (II) sulfate monohydrate ($MnSO_4.H_2O$) and sodium hydroxide (NaOH) was purchased from Sigma-Aldrich (Sigma-Aldrich Chemie GmbH, Taufkirchen, Germany). Boric acid (H_3BO_3) was supplied from Bandırma Boron Works (Eti Maden, Balıkesir, Turkey). Before the synthesis, the raw materials were verified by using PANalytical Xpert Pro XRD (PANalytical B.V., Almelo, the Netherlands). The details of the parameters used in the XRD analysis were Cu-Kα tube (λ =0.153 nm), voltage of 45 kV, current of 40 mA, step size 0.03°, step time 0.5 s, scan speed of 0.06 °C/s, and scan range of 7–90°. The patterns were matched with Inorganic Crystal Structure Database (ICSD).

The reactor, which used in the synthesis were explained in the previous studies[23-27]. After several pre-experiments, the raw material mole ratio was determined as 1:2:8 ($MnSO_4.H_2O$:NaOH: H_3BO_3). Hence, in the synthesis, 0.1262 mol of H_3BO_3 was dissolved in 25 mL of purified water (obtained from GFL 2004 (Gesellschaft für Labortechnik, Burgwedel, Germany)), then heated up to 90 °C and 0.0158 mol of $MnSO_4.H_2O$ and 0.0315 mol of NaOH were added and the lid of the reactor was closed. After the reaction time of 2 h, the slurry was filtered through chm F2044 grade (Ashless, slow filter speed) 90 mm blue ribbon filter paper (Chmlab, Barcelona, Spain) and the remaining contents on the filter paper were washed with purified water, in order to remove the unreacted raw materials and the byproduct of sodium sulfate (Na_2SO_4). Afterwards the filtrate was dried at 60 °C by EcoCELL LSIS-B2V/EC55 model incubator (MMM Medcenter Einrichtungen GmbH, Planegg, Germany). The expected reaction is given in (1):

$$MnSO_4.H_2O(s) + 2NaOH(s) + 8H_3BO_3(s) + xH_2O(aq) \rightarrow MnB_4O_7.yH_2O(s) + Na_2SO_4(aq) + 4H_3BO_3(aq) + zH_2O(aq) \quad \ldots (1)$$

Characterization of the product

In the XRD analysis the same aforementioned parameters were used. In the FTIR analysis, universal attenuated total reflectance (ATR) sampling accessory–Diamond/Zn is used with PerkinElmer Spectrum One (PerkinElmer, MA, USA). 4 scans were conducted with 4 cm^{-1} resolution within the scan range of 650–1800 cm^{-1}. Hitachi TM3030 Plus model SEM (Hitachi Ltd. Corporation, Tokyo, Japan) was used to study the morphology of the samples. In the analysis back scattered electron detector was used at the magnification of 5000X.

Thermal behavior of sample is studied in the temperature range of 40–520 °C with the heating rates of 2, 5, 10 and 20 °C/min under a nitrogen atmosphere, by use of PerkinElmer Diamond TG/DTA (PerkinElmer, MA, USA) thermal analysis instrument. Kinetic parameters such as activation energy (E_a) and exponential factor (k_o) were calculated by applying Coats-Redfern, Horowitz-Metzger and Van-Krevelen non-isothermal kinetic methods. In these methods, α is the degree of dehydration or conversion, R is the gas constant, n is the reaction order, T (K) is the absolute temperature, and β (K/min) is the heating rate.

In Coats-Redfern non-isothermal kinetic method; the E_a is obtained from the plot of $\ln[-\ln(1-\alpha)/T^2]$ as a function of 1/T for n = 1.0 or a plot of $\ln[(1-(1-\alpha)^{1-n})/(1-n)]$ as a function of 1/T for n ≠ 1. The Coats-Redfern kinetic method equations are given in Eqns 2 and 3:

$$\ln\left(-\frac{\ln(1-\alpha)}{T^2}\right) = \ln\left(\frac{k_0}{\beta E_a}\left(1-\frac{2RT}{E_a}\right)\right) - \frac{E_a}{RT} \quad (n=1) \quad \ldots (2)$$

$$\ln\left(-\frac{1-(1-\alpha)^{(1-n)}}{(1-n)T^2}\right) = \ln\left(\frac{k_0 R}{\beta E_a}\right) - \frac{E_a}{RT} \quad (n \neq 1) \quad \ldots (3)$$

In Horowitz-Metzger non-isothermal kinetic method, kinetic parameters were calculated by using the plot of conversion (α) as a function of temperature (T) of TG curves. The equation for Horowitz-Metzger method was given in Eqns 4 and 5. Temperature gradient (θ) can be explained with the T-T_s and T_s is defined as the temperature at which $(1-\alpha)_s=1/e=0.368$.

$$\ln(\ln(1-\alpha)) = \ln\left(\frac{k_0 R T_s^2}{\beta E_a}\right) - \frac{E_a}{RT_s} + \frac{E\theta}{RT_s^2} \quad (n=1) \quad \ldots (4)$$

$$\ln\left(\frac{1-(1-\alpha)^{(1-n)}}{1-n}\right) = \ln\left(\frac{k_0 RT_s^2}{\beta E_a}\right) - \frac{E_a}{RT_s^2} + \frac{E\theta}{RT_s^2} \quad (n \neq 1) \quad \ldots (5)$$

In Van-Krevelen non-isothermal kinetic method (Eqns 6 and 7), kinetic parameters were calculated by using the TG curves. E_a is obtained from the slope of the $\ln[-\ln(1-\alpha)]$ vs lnT plot for n = 1.0 or $\ln[(1-(1-\alpha)^{1-n})/(1-n)]$ vs lnT plot for $n \neq 1$.

$$\ln(-\ln(1-\alpha)) = \ln\left(\frac{k_0}{\beta}\left(\frac{E}{RT_{max}} + 1\right)^{-1}\left(\frac{0.368}{T_{max}}\right)^{\frac{E}{RT_{max}}}\right) - \left(\frac{E}{RT_{max}} + 1\right) lnT \ (n = 1) \quad \ldots (6)$$

$$\ln\left(\frac{1-(1-\alpha)^{(1-n)}}{1-n}\right) = \ln\left(\frac{k_0}{\beta}\left(\frac{E}{RT_{max}} + 1\right)^{-1}\left(\frac{0.368}{T_{max}}\right)^{\frac{E}{RT_{max}}}\right) - \left(\frac{E}{RT_{max}} + 1\right) lnT \ (n \neq 1) \quad \ldots (7)$$

Results and Discussion

XRD results of the synthesized manganese borates

XRD analysis was used to investigate crystallinity of synthesized manganese borate (Fig. 1). No distinct diffraction peaks proving the amorphous non-crystalline nature of the sample as shown in Fig. 1.

FTIR spectral analysis result of the synthesized manganese borates

The IR absorbance spectrum of synthesized manganese borate is shown in Fig. 2. According to FTIR spectrum, the peaks between 1743 cm^{-1} and 1454 cm^{-1} occured due to H-O-H bending [δ(H-O-H)]. The absorption peaks between 1415 cm^{-1} and 1288 cm^{-1} could be attributed to the asymmetric stretching of the three-coordinate boron to oxygen bands [$\nu_{as}(B_{(3)}\text{-}O)$]. The characteristic peak of boron-oxygen-hydrogen [δ(B-O-H)] bending was observed at 1199 cm^{-1}. The peak around 990 cm^{-1} could be arisen due to the symmetric stretching of the three-coordinate boron to oxygen bands [$\nu_s(B_{(3)}\text{-}O)$]. The bands between 866-682 cm^{-1} revealed the symmetric stretching of the four-coordinate boron to oxygen bands [$\nu_s(B_{(4)}\text{-}O)$]. The IR band at 634 cm^{-1} was characteristic peak of the three coordinate boron [δ(B-O-H)] bending.

SEM result of the synthesized manganese borates

The morphological properties of synthesized manganese borate were investigated by SEM analysis. As seen in Fig. 3, manganese borate samples had

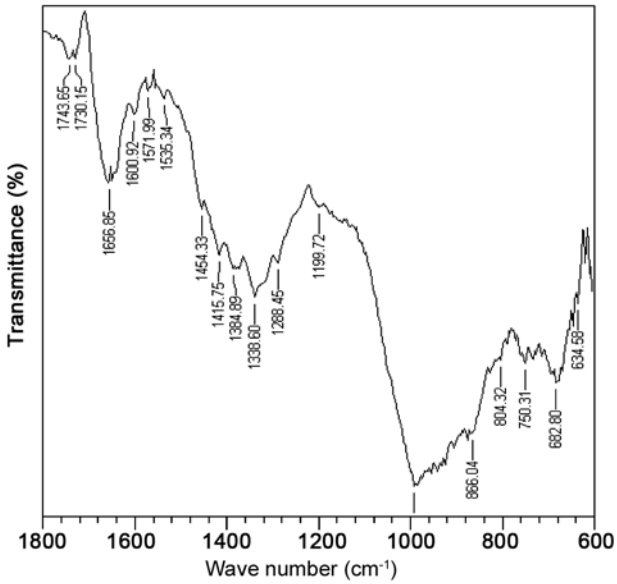

Fig. 2 — FTIR spectrum of synthesized manganese borate.

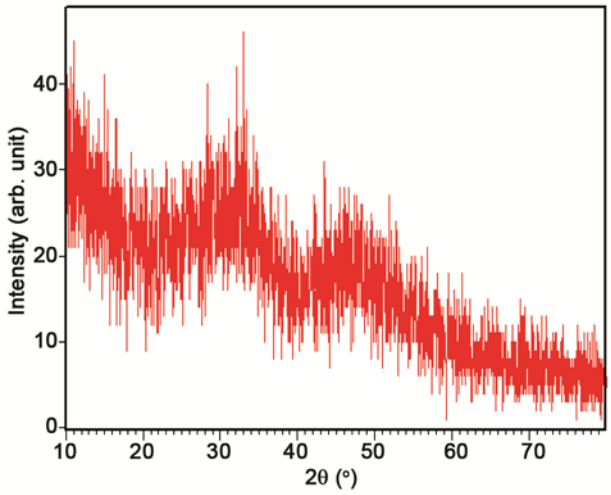

Fig. 1 — XRD pattern of synthesized manganese borate.

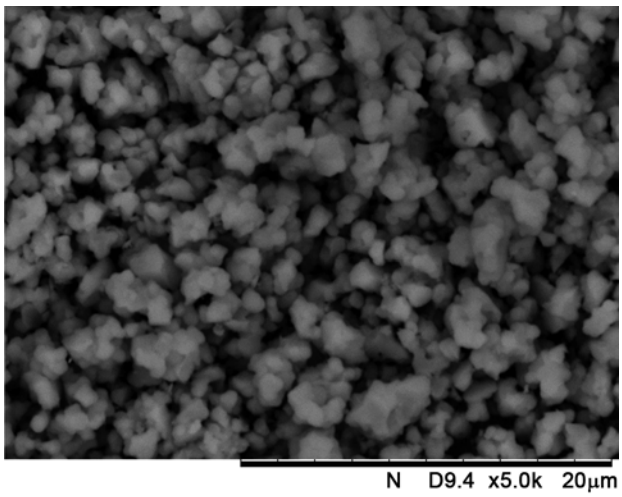

Fig. 3 — SEM of synthesized manganese borate.

uniform particle size distribution with micron scales which changed between 840 nm–1.96 μm. The obtained manganese borate particles had round particle shape and majorly agglomerated.

Thermal dehydration behavior and kinetic results

Thermal analyses results of the synthesized manganese borate are presented in Fig. 4. The dehydration process could be explained with the one-step reaction between the temperatures of 40–270 °C. Initial, final and peak temperatures of dehydration reaction for each heating rate are given in Table 1. In TG–DTG results, it is observed that the obtained weight losses at different heating rates were in compatible with each other and average of weight losses was determined as 19.26%.

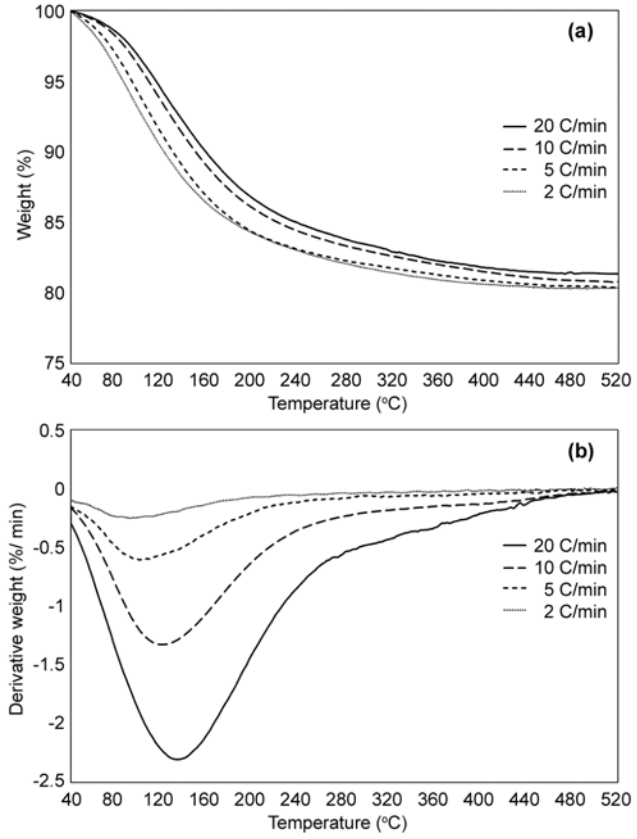

Fig. 4 — Thermal analyses results showing (a) TG and (b) DTG of the synthesized manganese borate.

Table 1 — Thermal analyses results of manganese borate

Heating Rate (°C/min)	$T_{initial}$ (°C)	T_{final} (°C)	T_{peak} (DTG) (°C)	w_{loss} (%)
2	42.09	171.41	94.43	19.60
5	42.56	201.63	99.74	19.56
10	43.20	235.74	119.15	19.24
20	43.44	271.64	134.21	18.64

The obtained weight loss indicated that the synthesized sample is manganese tetrahydric orthoborate ($MnH_4(BO_3)_2$) which was expressed in the study of Hartley and Ramage[5]. The probable decomposition reaction of $MnH_4(BO_3)_2$ (theoretical water content of 20.38% in the stoichiometric reaction) is given in Eqn 8:

$$2MnH_4(BO_3)_2 \xrightarrow{heat} MnB_4O_7 + MnO + 4H_2O \quad \ldots (8)$$

The kinetic parameters of dehydration mechanism were calculated using the Coats-Redfern, Horowitz-Metzger and Van-Krevelen non-isothermal kinetic methods between the conversion values of 0.03–0.995. Values of constants for each kinetic method are given in Table 2. According to the Table 2, the averages of activation energies for different heating rates were quite similar in each non-isothermal kinetic method.

In the Coats-Redfern method, the highest correlation coefficients (R^2) were calculated for the reaction order value of 1.5. Due to the highest R^2, Coats-Redfern kinetic method was selected as best fitted method for the dehydration reaction of manganese borate. For n = 1.5, the E_a and k_0 values were in the range of 30.24–41.15 kJ/mol and 2.16×10^3–5.68×10^3, respectively. In the Horowitz-Metzger method, the R^2 values were between 0.9742–0.9798 for n = 1.5. The E_a and k_0 values were in the range of 40.77–51.71 kJ/mol and 4.4×10^4–9.1×10^5, respectively. In the Van-Krevelen method, higher R^2 values obtained for the reaction order of 1.5 and the values were in the range of 0.9751–0.9915. The E_a and k_0 values were in the

Table 2 — Values of constants for each kinetic method

Method	β (K/min)	R^2	E_a (kJ/mol)	k_o
Coats-Redfern	20	0.9796	41.15	3.16×10^3
	10	0.9950	34.98	5.68×10^3
	5	0.9949	32.96	3.47×10^3
	2	0.9923	30.24	2.16×10^3
	$E_{average}$ (kJ/mol)		37.83	
Horowitz-Metzger	20	0.9742	40.77	4.4×10^4
	10	0.9775	45.73	1.6×10^5
	5	0.9787	47.94	3.3×10^5
	2	0.9798	51.71	9.1×10^5
	$E_{average}$ (kJ/mol)		46.54	
Van-Krevelen	20	0.9915	32.57	5.43×10^6
	10	0.9854	36.54	1.29×10^7
	5	0.9799	38.84	2.30×10^7
	2	0.9751	43.58	7.49×10^7
	$E_{average}$ (kJ/mol)		37.88	

range of 32.57–43.58 kJ/mol and 5.43×10^6–7.49×10^7, respectively.

Conclusions

In this study, a manganese borate of non-crystalline manganese tetrahydric orthoborate ($MnH_4(BO_3)_2$) was synthesized at the moderate conditions of 90 °C reaction temperature and 2 h reaction time from $MnSO_4.H_2O$, NaOH and H_3BO_3 by hydrothermal method. From the XRD results, it was seen that the synthesized compound was totally at amorphous phase. FTIR spectra of the products showed characteristic borate vibrations in the IR region and the SEM morphologies showed that compound was partially agglomerated with a uniform particle size distribution between 840 nm–1.96 μm. The dehydration process occurred in one-step reaction between the temperatures of 40–270 °C and average of weight loss was determined as 19.26%. Average activation energies were determined as 37.83, 46.54 and 37.88 kJ/mol for the non-isothermal kinetic methods of Coats-Redfern, Horowitz-Metzger and Van-Krevelen, respectively.

References

1 Das A P, Sukla L B, Pradhan N & Nayak S, *Biores Tech,* 102 (2011) 7381.
2 Nádaská G, Lesny J & Michalik I, *Health Environ J,* 100702-A (2010) 1.
3 Grygo-Szymanko E, Tobiasz A & Walas S, *Trends Anal Chem,* 80 (2016) 112.
4 Lewis R A, *Hawley's Condensed Chemical Dictionary*, 6th Edition, John Wiley & Sons, New Jersey (2016).
5 Hartley W N & Ramage H, *J Chem Soc,* 63 (1893) 129.
6 Neumair S C, Perfler L & Huppertz H, *Z Naturforsch B,* 66 (2011) 882.
7 Abrahams S C, Bernstein J L, Gibart P, Robbins M & Sherwood R C, *J Chem Phys,* 60 (1974) 1899.
8 Knyrim J S, Friedrichs J, Neumair S, Roeßner F, Floredo Y, Jakob S, Johrendt D & Huppertz H, *Solid State Sci,* 10 (2008) 168.
9 Yang D, Cong R, Gao W & Yang T J, *J Solid State Chem,* 201 (2013) 29.
10 Svirko L K & Boiko V F, *J Appl Spectrosc,* 19 (1973) 1208.
11 Norrestam R, Kritikos M & Sjödin A, *J Solid State Chem,* 114 (1995) 311.
12 Stoch L & Waclawska I, *Thermochim Acta,* 215 (1993) 273.
13 Ekmekyapar A, Baysar A & Kunkul A, *Ind Eng Chem Res,* 36 (1997) 3487.
14 Ekmekyapar A, Baysar A & Yuceer M J, *J Chem Eng Jpn,* 42 (2009) 478.
15 Erdogan Y, Zeybek A, Sahin A & Demirbas A, *Thermochim Acta,* 326 (1999) 99.
16 Koga N & Utsuoka T, *Thermochim Acta,* 443 (2006) 197.
17 Kanturk A, Sari M & Piskin S, *Korean J Chem Eng,* 25 (2008) 1331.
18 Kanturk A, Sari M & Piskin S, *Mater Charact,* 61 (2010) 640.
19 Yilmaz M S, Kanturk A & Piskin S, *Res Chem Intermed,* 41 (2015) 1893.
20 Derun E M & Senberber F T, *Sci World J,* (2014) 1.
21 Derun E M, Kipcak A S, Senberber F T & Yilmaz M S, *Res Chem Intermed,* 41 (2015) 853.
22 Kipcak A S, Senberber F T, Derun E M, Tugrul N & Piskin S, *Res Chem Intermed,* 41 (2015) 9129.
23 Asensio M O, Yildirim M, Senberber F T, Kipcak A S & Derun E M, *Res Chem Intermed,* 42 (2016) 4859.
24 Kipcak A S, Senberber F T, Yuksel S A, Derun E M & Piskin S, *Mater Res Bull,* 70, (2015) 442.
25 Kaplan A, Kipcak A S, Senberber F T, Derun E M & Piskin S, *Main Group Met Chem,* 38 (2015) 99.
26 Gurses P, Yildirim M, Kipcak A S, Yuksel S A, Derun E M & Piskin S, *Main Group Chem,* 14 (2015) 199.
27 Kipcak A S, Senberber F T, Yildirim M, Yuksel S A, Derun E M & Tugrul N, *Main Group Met Chem,* 39 (2016) 59.